

# Gemini Dark Matter

Andrew Cheek,<sup>1,2,\*</sup> Yu-Cheng Qiu,<sup>1,2,†</sup> and Liang Tan<sup>1,2,‡</sup>

<sup>1</sup>*Tsung-Dao Lee Institute & School of Physics and Astronomy, Shanghai Jiao Tong University, China*

<sup>2</sup>*Key Laboratory for Particle Astrophysics and Cosmology (MOE)*

*& Shanghai Key Laboratory for Particle Physics and Cosmology,  
Shanghai Jiao Tong University, Shanghai 200240, China*

(Dated: July 2, 2024)

The  $S_8/\sigma_8$  tension in the large scale structure can be explained by decaying dark matter with an almost degenerate spectrum and small enough decay width. Here we propose the Gemini dark matter model, which contains a heavy mother particle  $\chi_3$  and two twins  $\chi_{1/2}$  which are almost degenerate in mass and are produced at the same time. The dark sector is charged under the same Froggatt-Nielsen symmetry that can explain the hierarchy of the Standard model Yukawa couplings. The slightly heavier  $\chi_2$  decays into  $\chi_1$  and the axionic component of the flavon, which washes out the small scale structure and resolves  $S_8/\sigma_8$  tension. We present the production mechanism of Gemini dark matter and viable parameter regions. We find that despite the preferred dark matter mass being  $\mathcal{O}(1)\text{--}\mathcal{O}(100)$  keV, they constitute cold dark matter. The Gemini dark matter model predicts an abundance of dark radiation that will be probed in future measurements of the CMB.

## I. INTRODUCTION

The standard model of modern cosmology,  $\Lambda$ CDM model, currently provides a consistent picture of the observable Universe to a satisfying level of precision [1]. In recent years however, some observations have put tension on the  $\Lambda$ CDM [2] such as the Hubble tension and the  $S_8/\sigma_8$  tension [3]. If either of these tensions persist, cosmologists will have to go beyond  $\Lambda$ CDM. This paper focuses on a new physics solution to the  $S_8/\sigma_8$  tension.

Decaying dark matter (DDM) [4] has been proposed to resolve the  $S_8/\sigma_8$  tension [5–12]. The basic solution states that a cold dark matter (CDM) decays into a slightly lighter dark particle. The mass difference gives the product particle some velocity so it acts as warm dark matter (WDM), washing out structure a little. The decay lifetime should be  $\tau \sim \mathcal{O}(10)\text{--}\mathcal{O}(100)$  Gyr and the mass ratio between the decay product and the CDM quantified as  $\epsilon \equiv (m_{\text{CDM}}^2 - m_{\text{WDM}}^2)/2m_{\text{CDM}}^2$ , must be  $\sim 0.01\text{--}0.1$  [12]. This almost degenerate dark sector and highly suppressed decay must also evade indirect detection bounds. This could be achieved by assigning new quantum numbers and discrete symmetries.

The standard model (SM) of particle physics also contains several mysteries, and one of them is the mass hierarchy between three generations of quarks and leptons. One solution is the well-developed Froggatt-Nielsen (FN) mechanism [13–15], which introduces a chiral  $U(1)_{\text{FN}}$  (global or gauge) symmetry to the SM particles. This new symmetry forbids Yukawa terms at the renormalizable level. The dimension at which the Yukawa term appears at an effective nonrenormalizable level depends on the FN quantum numbers of the given particle. To re-

trieve the SM description, the  $U(1)_{\text{FN}}$  symmetry is spontaneously broken where the Yukawa couplings are now proportional to a common parameter,  $\lambda < 1$  to some positive generation-dependent power, and hierarchy emerges. This new symmetry is associated with a new scalar field, named flavon  $\Phi$ , and it mediates flavor-changing current, whose coupling strengths with fermions are proportional to the respective fermion masses. In other words, flavon couplings are generation-dependent.

The FN framework can be easily extended to the dark sector [16]. In the minimal setup, the dark sector interacts with the SM particles by mediating the flavon  $\Phi$ . Cosmologically, dark matter can be produced through either thermal freeze-out or non-thermal freeze-in [16–19]. Since the coupling between the flavon and the dark matter particle depends on dark matter mass, the direct and indirect detection may have interesting signatures.

Reference [17] considered DDM under the FN framework and suggested a potential model to resolve the  $S_8$ , albeit very roughly. In this paper, we systematically study the mass spectrum required to solve the  $S_8$  tension. We have identified a more consistent solution that results in different cosmology and phenomenological signals. In the dark sector, three dark fermions are charged under the FN symmetry. Two of them  $\chi_{1/2}$  are almost degenerate and the other one  $\chi_3$  is much heavier,  $m_3 \gg m_{1/2}$ . The decay channel  $\chi_2 \rightarrow \chi_1 + a$ , where  $a$  is the axionic component of the complex FN scalar  $\Phi$ , is responsible for resolving the  $S_8/\sigma_8$ . The  $\chi_{1/2}$  are produced from  $\chi_3$  decay,  $\chi_3 \rightarrow \chi_{1/2} + a$ . We name this model ‘Gemini dark matter’ (Gemini DM hereafter), where particles  $\chi_{1/2}$  are the twins and  $\chi_3$  is the mother particle. The mother particle is produced through freeze-in from the SM thermal bath. The preferred twin masses in this model are roughly  $\mathcal{O}(1)\text{--}\mathcal{O}(100)$  keV, and the average velocity of them is  $\sim 10^{-6}$ , which is cold despite its small mass.

The Gemini DM model predicts the existence of the dark radiation relic. During the parturition  $\chi_3 \rightarrow \chi_{1/2} + a$ , the light axionic flavon  $a$  is also produced as dark

\* [acheek@sjtu.edu.cn](mailto:acheek@sjtu.edu.cn)

† [ethanqiu@sjtu.edu.cn](mailto:ethanqiu@sjtu.edu.cn)

‡ [tanliang@sjtu.edu.cn](mailto:tanliang@sjtu.edu.cn)

radiation, which shall contribute to the deviation from neutrino effective number of species  $\Delta N_{\text{eff}}$ . It may be probed in future observations by CMB-S4 [20] and CMB-HD [21].

The paper goes as follows. Sec. II constructs the Gemini DM model. The cosmological production of Gemini DM is explained in Sec. III. Summary and discussions are in Sec. IV. Appendix A reviews the Froggatt-Nielsen mechanism in the SM sector.

## II. GEMINI DARK MATTER

In this section, we construct the Gemini DM model by extending the Froggatt-Nielsen symmetry to the dark sector, which contains Weyl fermions  $\chi_i$  carries FN charge  $n_i$ , which is also Standard Model gauge group singlet. There are three generations of  $\chi$ s. We focus on constructing a particle spectrum that resolves the  $S_8/\sigma_8$  tension, *i.e.* we require two particles with almost degenerate masses.

With our setup, below some UV cutoff scale  $\Lambda$ , the leading order nonrenormalizable operators that respect the global  $U(1)_{\text{FN}}$  appearing in the dark sector Lagrangian density are

$$\mathcal{L} \supset i\bar{\chi}_j \bar{\sigma}^\mu \partial_\mu \chi_j - \frac{\beta_{ij}}{2} \frac{\Phi^{n_i+n_j}}{\Lambda^{n_i+n_j-1}} \chi_i \chi_j + \text{h.c.}, \quad (1)$$

where  $\beta_{ij} \sim \mathcal{O}(1)$  are the coupling constants and  $\Phi$  is the flavon field is with FN charge  $-1$ . Here bar indicates the conjugate and  $\bar{\sigma}^\mu = (1, -\vec{\sigma})$ , where  $\vec{\sigma}$  is an array of Pauli matrices. The summation of dummy indices is employed here. The complex FN scalar  $\Phi$  can acquire a nontrivial vacuum expectation value (VEV),  $\langle \Phi \rangle = f_a$ , under its potential, leading to spontaneous symmetry breaking of  $U(1)_{\text{FN}}$ . Since we are considering the global  $U(1)_{\text{FN}}$ , and quantum gravity cannot accommodate such symmetries, it must be broken at least by the Planck scale [22, 23]. Therefore, the goldstone boson  $a$  (we call it axion for familiarity) acquires a mass through an explicit breaking term. After spontaneous symmetry breaking, the field can be written as  $\Phi = e^{ia/f_a} (f_a + \phi)/\sqrt{2}$ . A Taylor expansion gives

$$\left(\frac{\Phi}{\Lambda}\right)^n \rightarrow \lambda^n e^{ina/f_a} \left(1 + \frac{n\phi}{f_a} + \dots\right), \quad (2)$$

where the FN parameter is defined as  $\lambda \equiv f_a/\sqrt{2}\Lambda$ . The leading interaction terms in Eq.(1) are the Yukawa-type interactions that determine the  $\chi$  masses. After performing the phase rotation for each fermion,  $\chi_j \rightarrow e^{-in_j a/f_a} \chi_j$ , one rotates the axion away. This phase rotation generates couplings between  $\partial a$  and the  $\chi$ 's through the  $\Phi$  fields kinetic term. Using the equation of motion for the  $\chi$ 's, one obtains the interaction between  $a$  and fermions, due to the mismatch between mass eigenstates and coupling states, flavour changing currents that couple to flavon are still present. After diagonalizing the

mass matrix, interactions in Eq. (1) are expressed as

$$-\mathcal{L} \supset \frac{1}{2} m_k \chi_k \chi_k + g_{ij}^\phi \partial \chi_i \chi_j + g_{ij}^a \chi_i \chi_j + \text{h.c.}, \quad (3)$$

where  $m_k$  is the  $k$ -th diagonal component of  $D$  and

$$\begin{aligned} D &= \text{diag}(m_1, m_2, m_3) = U^\top M U \\ g_{ij}^\phi &= \frac{1}{2} \left[ \text{sym} \left( U^\top \frac{1}{f_a} \frac{\partial(\lambda M)}{\partial \lambda} U \right) \right]_{ij} \\ g_{ij}^a &= \left[ \text{sym} \left( \frac{ND}{f_a} \right) \right]_{ij} \\ M_{ij} &= \frac{1}{\sqrt{2}} f_a \beta_{ij} \lambda^{n_i+n_j-1} \\ N_{ij} &= (U^\dagger)_{ik} n_k U_{kj}. \end{aligned}$$

The  $U$  is a unitary matrix,  $UU^\dagger = 1$ . Here  $[\text{sym}(A)]_{ij} \equiv A_{ij} + A_{ji} - A_{ii} \delta_{ij}$ , for any matrix  $A$ . The presence of this symmetric sum for the off-diagonal couplings in  $g_{ij}^{\phi,a}$  is due to the spinor identity  $\chi_i \chi_j = \chi_j \chi_i$ . The nonvanishing flavor-changing couplings between flavons and  $\chi$  fields provide decay channels.

The Gemini DM model requires at least three generations of  $\chi$ . The reason is the following. In the minimal setup, we require the decay channel  $\chi_2 \rightarrow \chi_1 + a$  to resolve  $S_8$  tension. Meanwhile, the mass split between  $\chi_1$  and  $\chi_2$  is small, which is described by

$$\epsilon = \frac{1}{2} \left( 1 - \frac{m_1^2}{m_2^2} \right) \in (0.01, 0.1). \quad (4)$$

Recall that the mass matrix under the FN framework is approximately rank one. If only two generations are present, then one must have  $m_2 \gg m_1$ , which is not desirable. With three generations, one could have  $m_3 \gg m_2 \approx m_1$  under a reasonable choice of  $\beta_{ij}$ . In the Gemini DM model, we call  $\chi_3$  the mother particle and  $\chi_{1/2}$  the twins.

Here we present a specific parameter choice that gives us a desirable spectrum. We fix the FN parameter as  $\lambda = 0.171$  [24] as a benchmark model. The value of FN parameter  $\lambda$  has degeneracy with FN charge choices [25]. Choose the FN charge as

$$n_1 = 4.5 + n_3, \quad n_2 = 2.5 + n_3. \quad (5)$$

The charge  $n_3$  only determines the overall scale, which is irrelevant when determining couplings and mass ratios. The half charge can be absorbed by redefining the FN parameter. We parametrize  $\beta$  as

$$\beta = \begin{pmatrix} 1 & 1 & 1+c \\ 1 & 1 & 1 \\ 1+c & 1 & 1 \end{pmatrix}. \quad (6)$$

in order to obtain various spectra by varying the parameter  $c$  and determine how to produce the Gemini DM scenario. As shown in the upper panel of Fig. 1, for

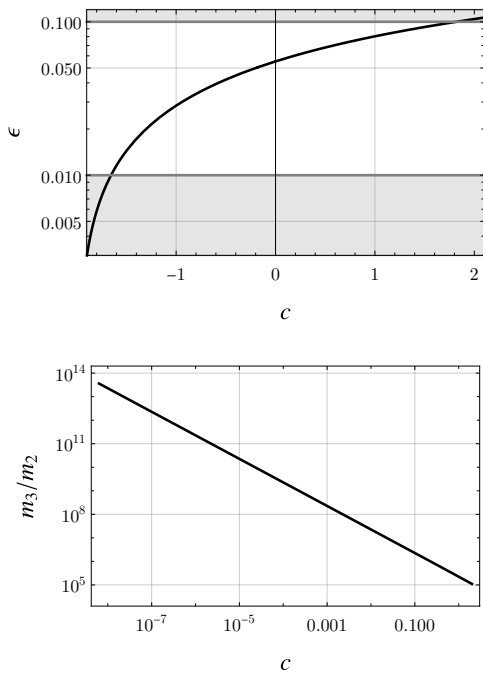


FIG. 1. The upper panel is the mass difference  $\epsilon$  between the twins  $\chi_{1/2}$  plotted against the single parameter  $c$  describes the  $\beta_{ij}$  in Eq. (6). The lower panel shows the mass ratio between the mother particle and the twins as a function of  $c$ .

$-1.7 \lesssim c \lesssim 2.0$ , one achieves the Gemini DM spectrum with an  $\epsilon$  that resolves the  $S_8$  tension using Eq. (3). Furthermore, the corresponding mass ratio of the much heavier mother particle  $\chi_3$  to the Gemini is shown in lower panel of Fig. 1.

We parametrize the flavon couplings in Eq. (3) as

$$\begin{aligned} g_{ij}^\phi &= \frac{1}{f_a} (m_i - m_j + m_i \delta_{ij}) \mathcal{A}_{ij} \\ g_{ij}^a &= \frac{1}{f_a} (m_i - m_j + m_i \delta_{ij}) \mathcal{B}_{ij}, \end{aligned} \quad (7)$$

where  $\mathcal{A}$  and  $\mathcal{B}$  are numerical matrices that are calculated explicitly with our choice of  $\beta$  (6) and FN charges (5). By varying  $c$ , one obtains a one-to-one correspondence between couplings and  $\epsilon$ . To determine the values and variance of the matrices  $\mathcal{A}$  and  $\mathcal{B}$  as shown in Table I, we perform the following method. We randomly sample  $c$ , adopting the uniform distribution as the prior, and select out those couplings associated with  $\epsilon \in (0.01, 0.1)$ . From these values we collect the corresponding  $\mathcal{A}$  and  $\mathcal{B}$ . We calculate the average and their deviations as shown in Table I. The result here is that the ranges of values in the matrices are not large compared to their central value. We can therefore justifiably treat them as constants for the following calculations.

Since  $\phi$  obtains its mass from the FN symmetry breaking,  $m_\phi$  is typically associated with the breaking scale  $f_a$ . The axion,  $a$ , is typically very light, obtaining its mass from some explicit breaking, which we treat as a free pa-

TABLE I. Statistics of matrix elements  $|\mathcal{A}_{ij}|^2$  and  $|\mathcal{B}_{ij}|^2$  under the parametrization Eq. (5), (6) and Eq. (7) with  $\epsilon \in (0.01, 0.1)$ , and randomly sampled  $c$  under uniform distribution. Central values are averages. The upper and the lower uncertainties indicate the maximum and the minimum.

$(ij)$	$ \mathcal{A}_{ij} ^2$	$ \mathcal{B}_{ij} ^2$
(11)	$6.64_{-0.47}^{+0.49} \times 10^3$	$48.6_{-0.4}^{+0.4}$
(22)	$6.76_{-0.48}^{+0.48} \times 10^3$	$49.4_{-0.4}^{+0.3}$
(33)	$1.57 \times 10^3 \pm 10^{-3}$	$12.3 \pm 10^{-5}$
(21)	$1.37 \times 10^2 \pm 10^{-1}$	$0.999_{-0.002}^{+0.001}$
(31)	$5.77_{-0.88}^{+0.95} \times 10^{-2}$	$4.21_{-0.65}^{+0.70} \times 10^{-4}$
(32)	$6.79_{-0.99}^{+1.11} \times 10^{-2}$	$4.98_{-0.75}^{+0.79} \times 10^{-4}$

parameter and  $m_a \ll m_{1/2}$ . In line with this thinking, we consider the case that  $\chi$  dominantly decays through  $a$ . With  $\chi_2$  slightly heavier than  $\chi_1$  ( $m_2 \gtrsim m_1$ ),  $\chi_3$  decays via  $\chi_{1/2} + a$  while  $\chi_2$  dominantly decays to  $\chi_1 + a$ . Heavy  $\phi$  decays into  $\chi$ s and  $a$ . These decay widths are given by

$$\begin{aligned} \Gamma_{\chi_i \rightarrow \chi_j a} &= \frac{m_i |g_{ij}^a|^2}{16\pi} \gamma_+ \left( \frac{m_j}{m_i}, \frac{m_a}{m_i} \right), \\ \Gamma_{\phi \rightarrow \chi_k \bar{\chi}_l} &= \frac{m_\phi |g_{ij}^\phi|^2}{8\pi(1 + \delta_{kl})} \gamma_- \left( \frac{m_k}{m_\phi}, \frac{m_l}{m_\phi} \right). \end{aligned} \quad (8)$$

Kinematics requires that  $m_i > m_j + m_a$  and  $m_\phi > m_k + m_l$ . The two-body decay phase space factor  $\gamma_\pm$  is

$$\begin{aligned} \gamma_\pm(y, z) &= (1 + y + z)^{3/2} (1 \pm y - z)^{3/2} \\ &\quad \times \sqrt{(1 - y + z)(1 \mp y - z)}, \end{aligned}$$

for any real number  $y$  and  $z$ . There are sub-dominant dark sector decays into SM particles mediated by  $\phi$  and  $a$ ,  $\chi_i \rightarrow \chi_j + \text{SM} + \text{SM}$ . However, it is a three-body decay, suppressed by at least another coupling squared  $\sim (m_{\text{SM}}/f_a)^2$ . So the three-body decay branching ratio (Br) is negligible.

Our twins are dark matter and the decay  $\chi_2 \rightarrow \chi_1 + a$  would give the lighter  $\chi_1$  enough kinetic energy to wash out some structures, which results in smaller  $S_8$  for the late universe. As long as the decay width is approximately

$$\Gamma_{\chi_2 \rightarrow \chi_1 a} = \frac{1}{\tau_8} \sim \mathcal{O}(10^{-43}) \text{ GeV}, \quad (9)$$

this decay resolves  $S_8/\sigma_8$  tension, equivalently,  $\tau_8 \sim \mathcal{O}(10)\text{--}\mathcal{O}(100)$  Gyr [12]. It is projected into a region on the  $f_a\text{--}m_{1/2}$  parameter space<sup>1</sup>. Choosing  $\epsilon = 0.05$

<sup>1</sup> Note that for  $\tau > 100$  Gyr, the model still works as a dark matter model without resolving the  $S_8$ . However, for  $\tau < 10$  Gyr, it has conflicts with other structure formation [12] constraints.

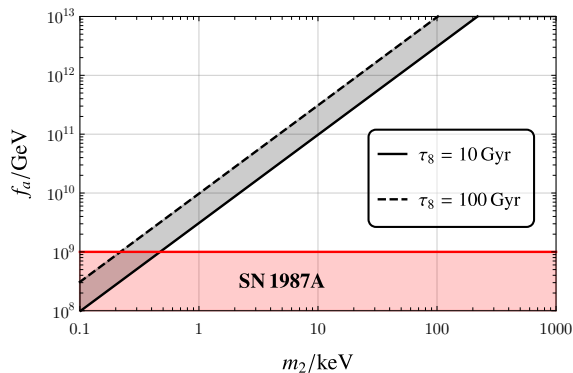


FIG. 2. Constraints on  $f_a$  and  $m_2$  parameter space. Here we choose the  $\epsilon = 0.05$  and  $m_a = 10^{-6}$  eV as the benchmark model. The gray stripe is the region that satisfies Eq. (9) and resolves  $S_8$  tension. The red region is excluded by the supernova axions [27].

and  $m_a = 10^{-6}$  eV as a benchmark model, the preferred parameter region could be parametrized as

$$m_{1/2} \approx 37 \times \left( \frac{f_a^2}{\tau_8} \right)^{1/3}, \quad (10)$$

which is the gray stripe shown in Fig. 2.

The axion mass  $m_a$  puts an upper bound on  $f_a$  via its overproduction from the misalignment mechanism. For  $m_a \sim 10^{-6}$  eV, this gives  $f_a < 1.1 \times 10^{13}$  GeV [26]. There is a lower bound on  $f_a$  in this figure. Our axion  $a$  couples to nucleons with a coupling of order  $\sim 1/f_a$ . This means that supernovas can emit a large axion flux, which is constrained as  $f_a > 10^9$  GeV by the Kamiokande-II neutrino detector at the time of SN 1987A [27]. Furthermore, the axion will couple to the photon via SM fermion loops, this coupling is highly suppressed  $g_{a\gamma} \sim m_a^2/f_a^2$ , avoids constraints by orders of magnitude [28] and leaves the axion stable on cosmological timescales. Note that with  $m_2 \sim 100$  keV the three-body  $\chi_2$  decay into charged fermions is kinematically forbidden not just suppressed. However, the  $\chi_2 \rightarrow \chi_1 + \gamma + \gamma$  decay occurs through a loop but has a decay width of  $\Gamma_{\chi_1 \rightarrow \chi_1 \gamma \gamma} \lesssim (m_2/f_a)^2 \Gamma_{\chi_2 \rightarrow \chi_1 a} \sim \mathcal{O}(10^{-48}) \text{ s}^{-1}$ , well below current limits [29].

The Gemini DM model has several parameters, among which  $\epsilon$  fixes the mass ratio between the twins, and  $\tau_8$  restricts  $m_{1/2}$  in terms of the breaking scale  $f_a$ . For now, we still have the mass of the mother particle  $m_3$  and the scale  $f_a$  undetermined. As long as  $m_a$  is small, it does not affect Gemini DM phenomenology. In the following section, we show that the production of Gemini DM in the early Universe will allow us to limit the  $f_a$  and  $m_3$  values that solve the  $S_8$  tension. This means that there is essentially only one free parameter, which is the  $f_a$ .

### III. COSMOLOGICAL PRODUCTION AND CONSTRAINTS

We propose a consistent production mechanism for the Gemini DM. The mother particle  $\chi_3$  freezes in through thermal  $\phi$  decay, and subsequently gives birth to the twins  $\chi_{1/2}$  via  $\chi_3 \rightarrow \chi_{1/2} + a$ . This mechanism could be divided into three stages, which are (1)  $\phi$  stays in thermal; (2)  $\phi$  decays into  $\chi_3$ ; and (3)  $\chi_3$  decays into  $\chi_1$  or  $\chi_2$ .

#### A. $\phi$ in thermal equilibrium with the Standard Model bath

From Fig. 2 one sees that current experiments require that at least  $f_a > 10^9$  GeV. Meanwhile, the  $m_\phi$  is generated from the potential that breaks the  $U(1)_{\text{FN}}$ . This means that  $m_\phi$  is much larger than the Higgs mass scale  $\sim \mathcal{O}(100)$  GeV. Furthermore, the SM thermal bath temperature required to produce appreciable quantities of  $\phi$  is much higher than the electroweak breaking scale. As reviewed in appendix A, at this scale, both  $\phi$  and  $a$  couple to SM particles through

$$n\lambda^n \frac{\phi}{f_a} \bar{Q}\mathcal{H}q, \quad n\lambda^n \frac{a}{f_a} \bar{Q}\mathcal{H}q, \quad (11)$$

where  $n = n_Q^{\text{FN}} + n_q^{\text{FN}}$  is the sum of the quark FN charges.  $\mathcal{H}$  is the SM Higgs doublet that does not carry an FN charge. We shall see that flavons enter the SM thermal bath through these interactions. Since we are interested in the temperature,  $T \sim \mathcal{O}(m_\phi)$ , we treat all SM particles as massless for simplicity. Focus on  $\phi$  for the moment. There are three different processes associated with this vertex, which are

$$\begin{aligned} \phi + \mathcal{H} &\rightarrow \bar{Q} + q, \\ \phi + Q &\rightarrow \mathcal{H} + q, \\ \phi + q &\rightarrow \mathcal{H} + Q. \end{aligned} \quad (12)$$

In the leading order, they are described as having the same amplitude, which is given by

$$|\mathcal{M}|^2 \approx \frac{\lambda^2}{f_a^2} (2p_Q p_q), \quad (13)$$

where  $p_j$  is the four-momentum of  $j$  particle. Here we have explicitly chosen  $n = 1$  because this will be the leading contribution. The other three particles, namely  $\{\mathcal{H}, Q, q\}$ , are in thermal equilibrium. The equilibrium number density  $n_j^{\text{eq}}$  can be approximated by integrating the Maxwell-Boltzmann distribution  $f_j^{\text{eq}} \approx e^{-E_j/T}$ ,

$$\begin{aligned} n_j^{\text{eq}} &= \frac{g_j}{(2\pi)^3} \int d^3 p_j f_j^{\text{eq}} \\ &= \frac{g_j}{2\pi^2} m_j^2 T K_2(m_j/T) \stackrel{m_j \rightarrow 0}{=} \frac{g_j}{\pi^2} T^3. \end{aligned} \quad (14)$$

Here  $g_j$  is the degree of freedom of  $j$  particle and  $m_j$  is its mass.  $T$  labels the temperature. The last approximation above takes the massless limit, which applies for  $\{\mathcal{H}, Q, q\}$ .  $K_\alpha(x)$  is the modified Bessel function of the second kind. The number density  $n_\phi$  evolution of  $\phi$  is governed by the Boltzmann equation, which includes three processes in Eq. (12) and their inverses,

$$\begin{aligned} \dot{n}_\phi + 3Hn_\phi &= -\tilde{\Gamma}_\phi (n_\phi - n_\phi^{\text{eq}}) \\ \tilde{\Gamma}_\phi &= \langle \sigma_{\mathcal{H}v} \rangle n_{\mathcal{H}}^{\text{eq}} + \langle \sigma_{Qv} \rangle n_Q^{\text{eq}} + \langle \sigma_{qv} \rangle n_q^{\text{eq}}, \end{aligned} \quad (15)$$

where  $\langle \sigma_{jv} \rangle$  labels the thermally averaged cross section of the process whose initial states are  $\phi$  and  $j$  particles. The  $H(T)$  is the Hubble parameter that describes the expansion of the universe. The interaction rate  $\tilde{\Gamma}_\phi(T)$  and the Hubble expansion rate  $3H(T)$  determines whether the  $\phi$  stays in the thermal equilibrium. Since at the relevant temperatures, the particles  $\{\mathcal{H}, Q, q\}$  are all massless, one can simplify the expression of  $\tilde{\Gamma}_\phi$  by performing a re-labeling of the integration variables in the second and third terms in  $\tilde{\Gamma}_\phi$ . This allows us to write

$$\begin{aligned} \tilde{\Gamma}_\phi &\approx \frac{1}{n_\phi^{\text{eq}}} \int \prod_j d\Pi_j \frac{\lambda^2}{f_a^2} (2p_Q p_q + 2p_{\mathcal{H}} p_q + 2p_Q p_{\mathcal{H}}) \\ &\times (2\pi)^4 \delta^4(p_\phi + p_{\mathcal{H}} - p_Q - p_q) e^{-(E_\phi + E_{\mathcal{H}})/T}, \end{aligned} \quad (16)$$

where the phase space integral is defined as  $d\Pi_j = g_j d^3 p_j / [(2\pi)^3 (2E_j)]$ , and  $j$  runs for all four particles in these processes. Following the method in Ref. [30], one converts the above formula into a single integration,

$$\begin{aligned} \tilde{\Gamma}_\phi &\approx \frac{g_{\mathcal{H}} g_Q g_q \lambda^2}{16(2\pi)^3} \frac{T^5}{f_a^2 m_\phi^2} \frac{\mathcal{I}(m_\phi/T)}{K_2(m_\phi/T)}, \\ \mathcal{I}(\zeta) &= \int_\zeta^\infty d\xi (\xi^2 - \zeta^2) (2\xi^2 - \zeta^2) K_1(\xi), \end{aligned} \quad (17)$$

where  $\zeta$  is a real number. Taking the standard cosmology picture we will assume that the Universe is dominated by radiation at early times. Then the Hubble parameter can be approximated by

$$H(T) \approx \frac{\pi}{3} \sqrt{\frac{g_\star}{10}} \frac{T^2}{M_{\text{Pl}}} \approx 3.4 \times \frac{T^2}{M_{\text{Pl}}}, \quad (18)$$

where  $M_{\text{Pl}} = 2.4 \times 10^{18}$  GeV is the reduced Planck scale and  $g_\star$  is the temperature-dependent effective number of energy degrees of freedom. To get the numerical expression we take  $g_\star(T \gtrsim T_{\text{EWSB}}) \approx 107$  [31].

To estimate when  $\phi$  decouples from the SM bath we compare  $\tilde{\Gamma}_\phi(T)$  and  $3H(T)$ . Similarly, this can be done for the  $a$  particle, and the interaction rate of (17) is modified by taking the massless limit

$$\tilde{\Gamma}_a \approx \frac{g_{\mathcal{H}} g_Q g_q \lambda^2 T^3}{(2\pi)^3 f_a^2}. \quad (19)$$

In Fig. 3 we show a specific realization where  $\tilde{\Gamma}_\phi > 3H$  for temperatures below the breaking scale  $f_a$ . We see

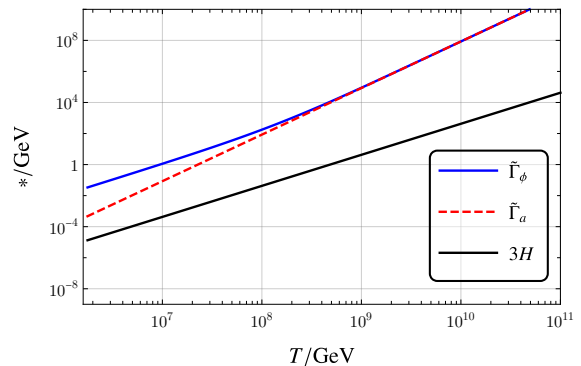


FIG. 3. Here we choose  $f_a = 2 \times 10^{10}$  GeV and  $m_\phi = 10^9$  GeV. The degrees of freedom are  $g_Q = 12$ ,  $g_q = 6$  and  $g_{\mathcal{H}} = 4$ . The FN charge is chosen as  $n = 1$  as the leading contribution, and the FN parameter is  $\lambda = 0.171$ . Note the red-dashed line, the interaction rate for the axion  $\tilde{\Gamma}_a$ , cross with the Hubble parameter at  $T_{\text{dec}}^a \approx 5 \times 10^4$  GeV under this choice of parameters.

that the axion interaction rate  $\tilde{\Gamma}_a$  follows the simple  $T^3$  dependence which, decreases in a cooling Universe faster than Hubble, this leads to an axion decoupling at around  $\sim 10^5$  GeV (left of the figure) [32]. Interestingly, for massive  $\phi$  the temperature dependence changes below  $T \sim m_\phi$  keeping it in equilibrium and its number density can be described by  $n_\phi^{\text{eq}}$ .

### B. $\chi_3$ freeze-in from $\phi$ decay

Given that there are parameter choices for our model that ensure that  $\phi$  stays in the thermal bath, we consider the standard freeze-in for  $\chi_3$  from  $\phi$  decay [33–38]. The Boltzmann equation for  $\chi_3$  is

$$\dot{n}_{\chi_3} + 3Hn_{\chi_3} = S(\phi \rightarrow \chi_3 \bar{\chi}_3), \quad (20)$$

where the source term is given by

$$\begin{aligned} S(\phi \rightarrow \chi_3 \bar{\chi}_3) &= g_\phi g_3^2 \int \frac{d^3 p_\phi}{(2\pi)^3} \frac{m_\phi}{E_\phi} \Gamma_{\phi \rightarrow \chi_3 \bar{\chi}_3} e^{-E_\phi/T} \\ &= \frac{g_\phi g_3^2}{2\pi^2} \Gamma_{\phi \rightarrow \chi_3 \bar{\chi}_3} m_\phi^2 T K_1(m_\phi/T). \end{aligned} \quad (21)$$

The decay width  $\Gamma_{\phi \rightarrow \chi_3 \bar{\chi}_3}$  is given by Eq. (8). In the second line, we have evaluated the integration explicitly. Following standard parametrization, we define the yield  $Y_3 = n_{\chi_3}/s$ , where  $s$  is the entropy density. The equilibrium condition of conservation of total entropy implies that  $ds/dt = -3sH$ . So the l.h.s. of the Boltzmann equation can be written as  $\dot{n}_{\chi_3} + 3Hn_{\chi_3} = sdY_3/dt$ . Furthermore, defining the variable  $x = m_\phi/T$  enables one to write  $dx/dt = -(x/T)(dT/dt) = xH$  for the radiation-dominated era. Then the Hubble parameter can be written as  $H(x) \approx 3.4 \times m_\phi^2/M_{\text{Pl}} x^2$ . Similarly, we extract out  $x$ -dependence in the entropy density,  $s \approx 27.3 \times s_0 m_\phi^3/T_0^3 x^3$ , where  $T_0 = 2.3 \times 10^{-13}$  GeV

is the CMB radiation temperature today. Therefore, the Boltzmann equation for  $\chi_3$  (20) becomes

$$\frac{dY_3}{dx} \approx \frac{g_\phi g_3^2}{186\pi^2} \frac{T_0^3 M_{\text{Pl}}}{s_0 m_\phi^2} \Gamma_{\phi \rightarrow \chi_3 \bar{\chi}_3} x^3 K_1(x), \quad (22)$$

which can be integrated directly, either numerically or taking  $\int_0^\infty x^3 K_1(x) = 3\pi/2$ . If we assume the initial yield of  $\chi_3$  is zero, we obtain the freeze-in yield of  $\chi_3$ ,

$$\begin{aligned} Y_3^{\text{f.i.}} &\approx Y_3(\infty) \approx \frac{3g_\phi g_3^2}{371\pi} \frac{T_0^3 M_{\text{Pl}}}{s_0 m_\phi^2} \Gamma_{\phi \rightarrow \chi_3 \bar{\chi}_3} \\ &\approx 0.32 \times \frac{T_0^3 M_{\text{Pl}}}{s_0 m_\phi} \frac{m_3^2}{f_a^2} \left(1 - \frac{4m_3^2}{m_\phi^2}\right)^{3/2}. \end{aligned} \quad (23)$$

In the last line, we use  $g_\phi = 1$  and  $g_3 = 2$  and take the numerical value for  $|\mathcal{A}_{33}|^2$  in the decay width from Table I.

### C. Relic $\chi_{1/2}$ from $\chi_3$ decay

In the Gemini DM model, dark matter consists of two twins, namely  $\chi_1$  and  $\chi_2$ . They are produced from  $\chi_3$  decay via  $\chi_3 \rightarrow \chi_{1/2} + a$ . One can write the relic yield of  $\chi_i$  as  $Y_i \approx \text{Br}(\chi_3 \rightarrow \chi_i a) Y_3^{\text{f.i.}}$  and we have  $Y_1 + Y_2 \approx Y_3^{\text{f.i.}}$ . The energy density today is given by  $\rho_i(T_0) = m_{1/2} Y_i s_0$ , where we have approximated  $m_1 \approx m_2 \approx m_{1/2}$ . Now the total relative relic density of the Gemini DM is given by

$$\begin{aligned} \Omega_{\text{DM}} h^2 &= \frac{(\rho_1 + \rho_2) h^2}{3M_{\text{Pl}}^2 H_0^2} \approx \frac{m_{1/2} Y_3^{\text{f.i.}} s_0 h^2}{3M_{\text{Pl}}^2 H_0^2} \\ &\approx 0.11 \times \frac{h^2 T_0^3 m_{1/2}}{H_0^2 M_{\text{Pl}} m_\phi} \frac{m_3^2}{f_a^2} \left(1 - \frac{4m_3^2}{m_\phi^2}\right)^{3/2}. \end{aligned} \quad (24)$$

To resolve the  $S_8$  tension, the decay width of  $\Gamma_{\chi_2 \rightarrow \chi_1 a}$  satisfying Eq. (9) puts a relation between  $m_{1/2}$  and  $f_a$ . For the benchmark model with  $\epsilon = 0.05$  and  $m_a = 10^{-6}$  eV (10), this gives

$$\begin{aligned} \Omega_{\text{DM}} h^2 &\approx 4.0 \times \frac{h^2 T_0^3 m_3^2}{H_0^2 M_{\text{Pl}} m_\phi (\tau_8 f_a^4)^{1/3}} \left(1 - \frac{4m_3^2}{m_\phi^2}\right)^{3/2} \\ &\approx 0.12 \left(\frac{m_3}{1.1 \times 10^4 \text{ GeV}}\right)^2 \left(\frac{f_a}{2 \times 10^{10} \text{ GeV}}\right)^{-4/3}, \end{aligned} \quad (25)$$

where the Hubble parameter today is  $H_0/h \approx 2.1 \times 10^{-42}$  GeV (from  $H_0 \equiv 100h$  km/s/Mpc) [39]. For the last line, we have chosen  $\tau_8 = 10$  Gyr, and  $m_\phi = 10^9$  GeV.

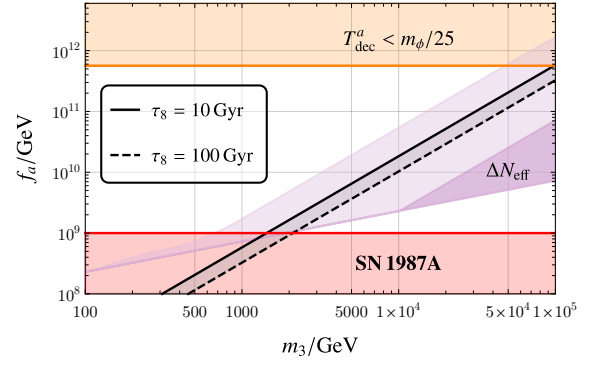


FIG. 4. Here we choose  $m_\phi = 10^9$  GeV and  $\Omega_{\text{DM}} h^2 = 0.12$  under the benchmark model,  $\epsilon = 0.05$  and  $m_a = 10^{-6}$  eV. The gray stripe is the parameter range that gives the correct relic and resolves  $S_8$ . The orange region is excluded by  $T_{\text{dec}}^a > m_\phi/25$ , and the red region is excluded by the supernova axions [27]. The darker purple region is excluded by overproduction of the dark radiation from  $\Delta N_{\text{eff}} < 0.276$  [1]. The lighter-purple region indicates  $\Delta N_{\text{eff}} > 0.04$  that can be covered for future CMB-S4 [20], whose sensitivity could reach  $\Delta N_{\text{eff}} \sim 0.02$ .

To give the correct relic that fits the cosmology, we should have  $\Omega_{\text{DM}} h^2 \approx 0.12$ . Figure 4 shows the allowed parameter space for  $f_a$  and  $m_3$  that resolves  $S_8$  and indicates the correct Gemini DM relic by the gray shaded strip. For a fixed  $m_\phi = 10^9$  GeV, we have a preferred  $f_a \sim \mathcal{O}(10^9)$ – $\mathcal{O}(10^{12})$  GeV, which indicates that the Gemini DM mass should be roughly  $m_{1/2} \sim \mathcal{O}(1)$ – $\mathcal{O}(100)$  keV, according to Fig. 2.

In addition to potential probes of this model from structure formation, the fact that the axion was once in thermal equilibrium means that axion relics will potentially be observable today. References [40–42] and others explore this possibility for the QCD axion. The greatest contribution will be by altering the number of relativistic degrees of freedom  $N_{\text{eff}}$  in the form of dark radiation. Deviations from the SM prediction ( $N_{\text{eff}})_{\text{SM}} \approx 3.044$  [43–48] are parameterised by

$$\Delta N_{\text{eff}} = \frac{8}{7} \left(\frac{11}{4}\right)^{4/3} \frac{\rho_a}{\rho_\gamma} \Big|_{T_{\text{rec}}}, \quad (26)$$

where  $\rho_\gamma$  is the photon energy density and  $T_{\text{rec}} \approx 0.26$  eV is the recombination temperature [49]. The energy density ratio is evaluated at the time of the recombination because measurements of the CMB give the most stringent constraints of  $\Delta N_{\text{eff}}$ . For example, the Planck collaboration gives  $(N_{\text{eff}})_{\text{P18}} = 2.88_{-0.42}^{+0.44}$  [1], which leads to  $\Delta N_{\text{eff}} = (N_{\text{eff}})_{\text{P18}} - (N_{\text{eff}})_{\text{SM}} \approx 0.276$ . The energy density of the thermal axion at decoupling is given by  $\rho_a^{\text{th}}(T_{\text{dec}}^a) = \rho_\gamma(T_{\text{dec}}^a)/2 = \pi^2(T_{\text{dec}}^a)^4/30$  where  $T_{\text{dec}}^a$  can be estimated by evaluating  $3H \approx \bar{\Gamma}_a$ . Using Eq. (19) one obtains  $T_{\text{dec}}^a \approx 300 f_a^2/M_{\text{Pl}}$ . The thermal axion's contri-

<sup>2</sup> The branching ratio can be approximated by using values for  $|\mathcal{B}_{ij}|^2$  in Table I. For example,  $\text{Br}(\chi_3 \rightarrow \chi_2 a) \approx |\mathcal{B}_{32}|^2/(|\mathcal{B}_{32}|^2 + |\mathcal{B}_{31}|^2)$ .

tribution to the  $\Delta N_{\text{eff}}$  is proportional to

$$\left. \frac{\rho_a^{\text{th}}}{\rho_\gamma} \right|_{T_{\text{rec}}} = \frac{1}{2} \left( \frac{g_{\star S}(T_{\text{rec}})}{g_{\star S}(T_{\text{dec}}^a)} \right)^{4/3}, \quad (27)$$

where  $g_{\star S}(T)$  is the relativistic degrees of freedom in entropy. This contribution has  $f_a$  dependence through  $T_{\text{dec}}^a$ . In the Gemini DM model, we require  $f_a > 10^9$  GeV (see Fig. 2), this translates to a  $\Delta N_{\text{eff}} \approx 0.028$ . As  $f_a$  increases, the decoupling temperature  $T_{\text{dec}}^a$  increases, which indicates a larger  $g_{\star S}(T_{\text{dec}}^a)$  and a smaller  $\Delta N_{\text{eff}}$ , with a minimum value of  $\approx 0.027$  assuming no extra BSM degrees of freedom in thermal equilibrium at early times. This constitutes a falsifiable prediction for the Gemini DM model because CMB probes of the next generation are expected to reach a sensitivity at or below this [20, 21]. Furthermore, there are two possible additional ways in which the axion energy density can be enhanced to levels that are already ruled out.

- (i) In addition to the decay that produces  $\chi_3$ , the  $\phi$  particle also decays into axion via  $\phi \rightarrow a + a$ . The decay term is generated from the kinetic term of  $\Phi$  and is therefore likely to dominate. As long as this decay occurs when  $a$  is still in thermal equilibrium, the effect will be washed out. The production from  $\phi$  decay continuously happens until  $n_\phi$  is exponentially suppressed when  $T \lesssim m_\phi/25$ . Therefore, as long as  $T_{\text{dec}}^a < m_\phi/25$ , there is no appreciable additional production of the dark radiation from  $\phi$  decay. Therefore, we avoid the overproduction of the dark radiation from  $\phi$  decay by putting an upper bound for  $f_a$ , indicated by the orange exclusion region in Fig 4.
- (ii) The decay  $\chi_3 \rightarrow \chi_{1/2} + a$  can also contribute to dark radiation. It occurs roughly at the temperature  $3H(T_3) \approx \Gamma_{\chi_3 \rightarrow \chi_{1/2} a}$ , which is,

$$T_3 \approx 9.9 \times 10^{-4} \frac{\sqrt{m_3^3 M_{\text{Pl}}}}{f_a}. \quad (28)$$

For the parameter space that we are interested in, we usually have  $T_3 < T_{\text{dec}}^a$ . So this extra contribution could not be avoided. To estimate the additional contribution we assume instantaneous decay, *i.e.*  $\Delta\rho_a(T_3) \approx m_3 Y_3^{\text{f.i.}S}(T_3)/2$ , where the half indicates the energy sharing between  $\chi_{1/2}$  and  $a$ . This gives an additional contribution to the  $\Delta N_{\text{eff}}$  at the recombination, which is proportional to

$$\begin{aligned} \left. \frac{\Delta\rho_a}{\rho_\gamma} \right|_{T_{\text{rec}}} &= \frac{\Delta\rho_a(T_3)}{\rho_\gamma(T_{\text{rec}})} \left( \frac{T_{\text{rec}}}{T_3} \right)^4 \left( \frac{g_{\star S}(T_{\text{rec}})}{g_{\star S}(T_3)} \right)^{4/3} \\ &\approx 6.9 \times 10^6 \frac{T_3}{m_\phi} \left( \frac{g_{\star S}(T_{\text{rec}})}{g_{\star S}(T_3)} \right)^{4/3}, \end{aligned} \quad (29)$$

where we have neglected the phase space factor from Eq. (8) in the second line since we are mostly interested in the limit  $m_\phi \gg m_3$ . This energy density ratio

depends on  $m_3$  and  $f_a$  through  $T_3$  given in Eq. (28). The constraint demands an upper bound of this ratio, which is translated to a lower bound on  $f_a$  in terms of  $m_3$ .

Therefore, the total radiation  $\rho_a = \rho_a^{\text{th}} + \Delta\rho_a$  at recombination gives an  $\Delta N_{\text{eff}}$  that proportional to the sum of Eq. (27) and (29). We show a region in Fig. 4 that is excluded by current CMB results on  $\Delta N_{\text{eff}} > 0.276$  reported by Planck [1]. Once again, the above calculation requires  $T_{\text{dec}}^a > T_3$ , otherwise, the decay axions are thermalised and  $\Delta N_{\text{eff}} \approx 0.027$ . This is the reason the low  $f_a$  region is not covered by  $\Delta N_{\text{eff}}$  constraint in Fig. 4. We have additionally shaded a region in light purple which shows where  $\Delta N_{\text{eff}} > 0.04$ , we do this to show the level of sensitivity future CMB probes will require in order to rule out this solution to the  $S_8$  tension.

Dark matter models produced from thermal processes at the with  $m_{\text{DM}} \sim \mathcal{O}(10)$  keV are typically highly constrained by inferring the matter power spectrum through measurements of the Lyman- $\alpha$  forest [50, 51]. To see whether the WDM constraint applies, one has to estimate the free-streaming scale. In the instantaneous decay approximation of the process  $\chi_3 \rightarrow \chi_{1/2} + a$ , the twins  $\chi_{1/2}$  obtain the average momentum  $\langle p \rangle_3 \approx m_3/2$  at temperature  $T_3$  (28). This momentum is redshifted to today and becomes  $\langle p \rangle_0$ , rendering the twins non-relativistic. Their average velocity today can be expressed as,

$$\begin{aligned} \langle v \rangle_0 &\approx \frac{\langle p \rangle_0}{m_{1/2}} \approx \frac{m_3}{2m_{1/2}} \frac{T_0}{T_3} \left( \frac{g_{\star S}(T_0)}{g_{\star S}(T_3)} \right)^{1/3} \\ &\approx 1.4 \times 10^{-6} \left( \frac{m_\phi}{10^9 \text{ GeV}} \right)^{-1/4}. \end{aligned} \quad (30)$$

For the last approximation, we have evaluated the number under the benchmark model applying Eq. (10) and Eq. (24) with fixed  $\Omega_{\text{DM}} h^2 = 0.12$  and  $\tau_8 = 10$  Gyr, which corresponds to the parameters located in the gray strip in Fig. 4. The dependence on  $m_3$  and  $f_a$  canceled out after assuming that  $m_3 \ll m_\phi$ . The dependence on  $m_\phi$  is weak. This indicates that the Gemini DM is typically very cold today. With this result, we can estimate the free-streaming scale of the Gemini DM, which is

$$\lambda_{\text{fs}} \approx \frac{\langle v \rangle_0}{H_0} \approx 4.1 \times 10^{-3} \text{ Mpc}/h. \quad (31)$$

This free-streaming scale is much smaller than  $\mathcal{O}(1)$  Mpc, the scale of Ly- $\alpha$  matter power spectrum [52]. Hence, the usual keV WDM constraint [53] does not apply to Gemini DM [54, 55].

#### IV. SUMMARY AND DISCUSSION

In this work, we construct a decaying dark matter model, named Gemini DM, that resolves the  $S_8/\sigma_8$  tension in the large-scale structure, by extending a consistent Froggatt-Nielsen symmetry, that explains the

fermion mass hierarchy, to the dark sector. Our model consists of three generations of dark fermions, among which two of them have almost degenerate mass (the twins) and the other one (the mother) is much heavier. The twins are the main dark matter component today and the mother particle gives birth to them through its decay. The production mechanisms of the mother particle is nonthermal freeze-in from the Standard Model thermal bath. We have the mass of the twins roughly  $m_{1/2} \sim \mathcal{O}(\text{keV})$ , which is small. However, because they never thermalize and are produced via  $\chi_3$  decay, they constitute a cold dark matter model. Dark radiation is also produced during the production of the Gemini DM, which is the prediction of our model. This radiation is expected to be probed for future CMB observations.

Unlike the usual DDM solution to the  $S_8$  tension, only a fraction of the total dark matter decays. This will likely alter the required  $\epsilon \in (0.01, 0.1)$ , but not by much, for the following reason. The cold dark matter decays into warm dark matter and suppresses structure formation below the free-streaming scale  $k_{\text{fs}}^{-1}$ . This suppression follows the relation  $\delta_{\text{WDM}} \approx (k_{\text{fs}}^2/k^2)\delta_{\text{CDM}}$  [56], where the free-streaming scale is proportional to the particle velocity, determined by the mass separation, *i.e.*,  $k_{\text{fs}}^{-1} \propto \epsilon$ . If WDM is produced from only a fraction of the total dark matter, the suppression of structure formation is  $f_{\text{W}}\delta_{\text{WDM}} \propto f_{\text{W}}k_{\text{fs}}^2 \propto f_{\text{W}}/\epsilon^2$ , where  $f_{\text{W}}$  is the fraction of WDM relative to the total DM. This implies that a smaller fraction of DDM requires a larger energy release to achieve the same level of structure suppression. Therefore, the required mass-splitting factor is  $\epsilon' \equiv \epsilon/\sqrt{f_{\text{W}}}$ . For Gemini DM, where  $f_{\text{W}} \approx 0.5$ , this requires  $\sqrt{2}$  times the energy compared to the previously favored  $\epsilon$  in [12]. Hence, adopting  $\epsilon = 0.05$  for our benchmark model in the main text is reasonable.

One may attempt to identify the Gemini DM as the sterile neutrino. This could be achieved by considering the additional coupling between lepton and  $\chi$  particles. After the seesaw mechanism, one ends up with a suppressed neutrino mass matrix and a heavy dark sector. We leave this for future study.

If the  $S_8$  tension persists and the next generation of CMB measurements find an indication of additional relativistic degrees of freedom  $\Delta N_{\text{eff}} \approx 0.027$ , we will have a strong candidate solution to both simultaneously in the Gemini DM model.

## ACKNOWLEDGMENTS

We thank Yong Du, Jie Sheng, Chuan-Yang Xing, and Jiang Zhu for their valuable discussions. The authors are supported by the National Natural Science Foundation of China (12375101, 12090060 and 12090064) and the SJTU Double First Class start-up fund (WF220442604).

TABLE II. FN charge assignment of quarks and leptons.

Generation $i$	$\bar{Q}_L$	$u_R$	$d_R$	$\bar{\ell}_L$	$e_R$	$\Phi$
1	3	4	1	1	4	
2	2	1.5	0	0.5	1	-1
3	0	0	0	0	0	

## Appendix A: Review on Froggatt-Nielsen mechanism

The FN mechanism explains the SM fermion hierarchy via the introduction of an extra chiral  $U(1)_{\text{FN}}$  symmetry under some energy scale, which could be either global or gauged. For simplicity, we adopt the global symmetry here. We follow the Ref. [24], and one typical  $U(1)_{\text{FN}}$  charge assignment of the SM fermions is presented in Table II. Since FN charges are assigned for SM particles, the usual Yukawa interactions are forbidden by  $U(1)_{\text{FN}}$ . The leading order terms that give fermion mass are non-renormalizable. These non-renormalizable operators generate interactions between fermions and flavons. We review the FN framework by describing how it works in the lepton sector, the quark sector can be derived in the same way. Below some UV cutoff scale  $\Lambda$ , the leading order operators are

$$-\mathcal{L} \supset g_{ij} \left( \frac{\Phi}{\Lambda} \right)^{n_{\ell}^{ij}} \bar{\ell}_L^i \mathcal{H} e_R^j + \text{h.c.}, \quad (\text{A1})$$

where  $\mathcal{H}$  is the Higgs doublet and it does not carry an FN charge.  $g_{ij}$  is some order 1 coupling that is not responsible for the hierarchy.  $n_{\ell}^{ij} = n_{\ell}^i + n_{\ell}^j$  is the lepton FN charge matrix, where  $n_{\ell}^i$  and  $n_{\ell}^j$  are FN charges of  $\bar{\ell}_L^i$  and  $e_R^j$  respectively. Explicitly,

$$n_{\ell} = \begin{pmatrix} 5 & 2 & 1 \\ 4.5 & 1.5 & 0.5 \\ 4 & 1 & 0 \end{pmatrix}. \quad (\text{A2})$$

Note that here the half charge could be absorbed by redefining the FN parameter. After the spontaneous symmetry breaking of  $U(1)_{\text{FN}}$  by  $\Phi$ , we can do the same field expansion as Eq. (2). After performing the same phase rotation as described in Sec. (II), the leading term in Eq.(A1) would be the usual Yukawa interactions. The Yukawa matrix of the charged leptons is now hierarchically textured,

$$y_{\ell} \sim \begin{pmatrix} \mathcal{O}(\lambda^5) & \mathcal{O}(\lambda^2) & \mathcal{O}(\lambda^1) \\ \mathcal{O}(\lambda^{4.5}) & \mathcal{O}(\lambda^{1.5}) & \mathcal{O}(\lambda^{0.5}) \\ \mathcal{O}(\lambda^4) & \mathcal{O}(\lambda^1) & \mathcal{O}(1) \end{pmatrix}, \quad (\text{A3})$$

where  $\lambda \approx 0.171$  could give rise to a hierarchy between three generations and provide the best fit with the observation [24]. Therefore, after the electroweak symmetry breaking  $\mathcal{H} \rightarrow \langle \mathcal{H} \rangle$ , one obtains lepton masses and

interactions with the flavon field,

$$-\mathcal{L} \supset m_k \bar{e}_L^k e_R^k + g_{e,ij}^\phi \phi \bar{e}_L^i e_R^j + g_{e,ij}^a a \bar{e}_L^i e_R^j + \text{h.c.} . \quad (\text{A4})$$

Here we have rotated in the lepton mass eigenstates. In this basis, one obtains the relation

$$g_{e,ij} \propto \frac{m_i - m_j + m_i \delta_{ij}}{f_a} ,$$

which is characteristic of the FN framework. The diagonal couplings between flavon and fermions are propor-

tional to fermion mass, and the off-diagonal couplings are determined by their mass difference. The quarks couples to flavons basically in the same way as the charged leptons with up to slightly different constants. Note that neutrino mass could be generated through dim-5 operator [57, 58] in the SM effective field theory. This operator should also be modified under the FN framework [24], which gives rise to neutrino masses and interactions with flavons in a similar manner.

- 
- [1] **Planck** Collaboration, N. Aghanim *et al.*, “*Planck 2018 results. VI. Cosmological parameters*,” *Astron. Astrophys.* **641** (2020) A6, [[arXiv:1807.06209](#) [astro-ph.CO]]. [Erratum: *Astron. Astrophys.* 652, C4 (2021)].
- [2] E. Abdalla *et al.*, “*Cosmology intertwined: A review of the particle physics, astrophysics, and cosmology associated with the cosmological tensions and anomalies*,” *JHEAp* **34** (2022) 49–211, [[arXiv:2203.06142](#) [astro-ph.CO]].
- [3] E. Di Valentino *et al.*, “*Cosmology Intertwined III:  $f\sigma_8$  and  $S_8$* ,” *Astropart. Phys.* **131** (2021) 102604, [[arXiv:2008.11285](#) [astro-ph.CO]].
- [4] M. S. Turner, “*Cosmology with Decaying Particles*,” *Phys. Rev. D* **31** (1985) 1212.
- [5] S. Aoyama, T. Sekiguchi, K. Ichiki, and N. Sugiyama, “*Evolution of perturbations and cosmological constraints in decaying dark matter models with arbitrary decay mass products*,” *JCAP* **07** (2014) 021, [[arXiv:1402.2972](#) [astro-ph.CO]].
- [6] K. Enqvist, S. Nadathur, T. Sekiguchi, and T. Takahashi, “*Decaying dark matter and the tension in  $\sigma_8$* ,” *JCAP* **09** (2015) 067, [[arXiv:1505.05511](#) [astro-ph.CO]].
- [7] G. Franco Abellán, R. Murgia, V. Poulin, and J. Lavalle, “*Implications of the  $S_8$  tension for decaying dark matter with warm decay products*,” *Phys. Rev. D* **105** no. 6, (2022) 063525, [[arXiv:2008.09615](#) [astro-ph.CO]].
- [8] G. Franco Abellán, R. Murgia, and V. Poulin, “*Linear cosmological constraints on two-body decaying dark matter scenarios and the  $S_8$  tension*,” *Phys. Rev. D* **104** no. 12, (2021) 123533, [[arXiv:2102.12498](#) [astro-ph.CO]].
- [9] T. Simon, G. Franco Abellán, P. Du, V. Poulin, and Y. Tsai, “*Constraining decaying dark matter with BOSS data and the effective field theory of large-scale structures*,” *Phys. Rev. D* **106** no. 2, (2022) 023516, [[arXiv:2203.07440](#) [astro-ph.CO]].
- [10] L. Fuß and M. Garny, “*Decaying Dark Matter and Lyman- $\alpha$  forest constraints*,” *JCAP* **10** (2023) 020, [[arXiv:2210.06117](#) [astro-ph.CO]].
- [11] J. Bucko, S. K. Giri, F. H. Peters, and A. Schneider, “*Probing the two-body decaying dark matter scenario with weak lensing and the cosmic microwave background*,” *Astron. Astrophys.* **683** (2024) A152, [[arXiv:2307.03222](#) [astro-ph.CO]].
- [12] L. Fuß, M. Garny, and A. Ibarra, “*Minimal decaying dark matter: from cosmological tensions to neutrino signatures*,” [[arXiv:2403.15543](#) [hep-ph]].
- [13] C. D. Froggatt and H. B. Nielsen, “*Hierarchy of Quark Masses, Cabibbo Angles and CP Violation*,” *Nucl. Phys. B* **147** (1979) 277–298.
- [14] M. Leurer, Y. Nir, and N. Seiberg, “*Mass matrix models: The Sequel*,” *Nucl. Phys. B* **420** (1994) 468–504, [[arXiv:hep-ph/9310320](#)].
- [15] M. Leurer, Y. Nir, and N. Seiberg, “*Mass matrix models*,” *Nucl. Phys. B* **398** (1993) 319–342, [[arXiv:hep-ph/9212278](#)].
- [16] L. Calibbi, A. Crivellin, and B. Zaldívar, “*Flavor portal to dark matter*,” *Phys. Rev. D* **92** no. 1, (2015) 016004, [[arXiv:1501.07268](#) [hep-ph]].
- [17] A. Cheek, J. K. Osiński, L. Roszkowski, and S. Trojanowski, “*Dark matter production through a non-thermal flavon portal*,” *JHEP* **03** (2023) 149, [[arXiv:2211.02057](#) [hep-ph]].
- [18] K. S. Babu, S. Chakdar, N. Das, D. K. Ghosh, and P. Ghosh, “*FIMP dark matter from flavon portals*,” *JHEP* **07** (2023) 143, [[arXiv:2305.03167](#) [hep-ph]].
- [19] R. Mandal and T. Tong, “*Exploring freeze-out and freeze-in dark matter via effective Froggatt-Nielsen theory*,” *JCAP* **11** (2023) 074, [[arXiv:2307.14972](#) [hep-ph]].
- [20] **CMB-S4** Collaboration, K. N. Abazajian *et al.*, “*CMB-S4 Science Book, First Edition*,” [[arXiv:1610.02743](#) [astro-ph.CO]].
- [21] **CMB-HD** Collaboration, S. Aiola *et al.*, “*Snowmass2021 CMB-HD White Paper*,” [[arXiv:2203.05728](#) [astro-ph.CO]].
- [22] T. Banks and N. Seiberg, “*Symmetries and Strings in Field Theory and Gravity*,” *Phys. Rev. D* **83** (2011) 084019, [[arXiv:1011.5120](#) [hep-th]].
- [23] M. Reece, “*TASI Lectures: (No) Global Symmetries to Axion Physics*,” *PoS TASI2022* (2024) 008, [[arXiv:2304.08512](#) [hep-ph]].
- [24] Y.-C. Qiu, J.-W. Wang, and T. T. Yanagida, “*Predictions of  $m_{ee}$  and neutrino mass from a consistent Froggatt-Nielsen model*,” *Phys. Rev. D* **108** no. 11, (2023) 115021, [[arXiv:2307.16470](#) [hep-ph]].
- [25] M. Fedele, A. Mastroddi, and M. Valli, “*Minimal Froggatt-Nielsen textures*,” *JHEP* **03** (2021) 135, [[arXiv:2009.05587](#) [hep-ph]].
- [26] L. Hui, “*Wave Dark Matter*,” *Ann. Rev. Astron. Astrophys.* **59** (2021) 247–289, [[arXiv:2101.11735](#)].

- [astro-ph.CO]].
- [27] A. Lella, P. Carena, G. Co', G. Lucente, M. Giannotti, A. Mirizzi, and T. Rauscher, "Getting the most on supernova axions," *Phys. Rev. D* **109** no. 2, (2024) 023001, [[arXiv:2306.01048](#) [hep-ph]].
- [28] C. B. Adams *et al.*, "Axion Dark Matter," in *Snowmass 2021*. 3, 2022. [[arXiv:2203.14923](#) [hep-ex]].
- [29] F. Calore, A. Dekker, P. D. Serpico, and T. Siebert, "Constraints on light decaying dark matter candidates from 16 yr of INTEGRAL/SPI observations," *Mon. Not. Roy. Astron. Soc.* **520** no. 3, (2023) 4167–4172, [[arXiv:2209.06299](#) [hep-ph]].
- [30] P. Gondolo and G. Gelmini, "Cosmic abundances of stable particles: Improved analysis," *Nucl. Phys. B* **360** (1991) 145–179.
- [31] M. Drees, F. Hajkarim, and E. R. Schmitz, "The Effects of QCD Equation of State on the Relic Density of WIMP Dark Matter," *JCAP* **06** (2015) 025, [[arXiv:1503.03513](#) [hep-ph]].
- [32] B. Lillard, M. Ratz, T. Tait, M. P., and S. Trojanowski, "The Flavor of Cosmology," *JCAP* **07** (2018) 056, [[arXiv:1804.03662](#) [hep-ph]].
- [33] J. McDonald, "Thermally generated gauge singlet scalars as selfinteracting dark matter," *Phys. Rev. Lett.* **88** (2002) 091304, [[arXiv:hep-ph/0106249](#)].
- [34] A. Kusenko, "Sterile neutrinos, dark matter, and the pulsar velocities in models with a Higgs singlet," *Phys. Rev. Lett.* **97** (2006) 241301, [[arXiv:hep-ph/0609081](#)].
- [35] K. Petraki and A. Kusenko, "Dark-matter sterile neutrinos in models with a gauge singlet in the Higgs sector," *Phys. Rev. D* **77** (2008) 065014, [[arXiv:0711.4646](#) [hep-ph]].
- [36] L. J. Hall, K. Jedamzik, J. March-Russell, and S. M. West, "Freeze-In Production of FIMP Dark Matter," *JHEP* **03** (2010) 080, [[arXiv:0911.1120](#) [hep-ph]].
- [37] N. Bernal, M. Heikinheimo, T. Tenkanen, K. Tuominen, and V. Vaskonen, "The Dawn of FIMP Dark Matter: A Review of Models and Constraints," *Int. J. Mod. Phys. A* **32** no. 27, (2017) 1730023, [[arXiv:1706.07442](#) [hep-ph]].
- [38] M. Bauer and T. Plehn, *Yet Another Introduction to Dark Matter: The Particle Physics Approach*, vol. 959 of *Lecture Notes in Physics*. Springer, 2019. [[arXiv:1705.01987](#) [hep-ph]].
- [39] **Particle Data Group** Collaboration, R. L. Workman *et al.*, "Review of Particle Physics," *PTEP* **2022** (2022) 083C01.
- [40] M. S. Turner, "Thermal Production of Not SO Invisible Axions in the Early Universe," *Phys. Rev. Lett.* **59** (1987) 2489. [Erratum: *Phys.Rev.Lett.* 60, 1101 (1988)].
- [41] A. Salvio, A. Strumia, and W. Xue, "Thermal axion production," *JCAP* **01** (2014) 011, [[arXiv:1310.6982](#) [hep-ph]].
- [42] F. D'Ermo, F. Hajkarim, and S. Yun, "Thermal QCD Axions across Thresholds," *JHEP* **10** (2021) 224, [[arXiv:2108.05371](#) [hep-ph]].
- [43] G. Mangano, G. Miele, S. Pastor, and M. Peloso, "A Precision calculation of the effective number of cosmological neutrinos," *Phys. Lett. B* **534** (2002) 8–16, [[arXiv:astro-ph/0111408](#)].
- [44] P. F. de Salas and S. Pastor, "Relic neutrino decoupling with flavour oscillations revisited," *JCAP* **07** (2016) 051, [[arXiv:1606.06986](#) [hep-ph]].
- [45] S. Gariazzo, P. F. de Salas, and S. Pastor, "Thermalisation of sterile neutrinos in the early Universe in the 3+1 scheme with full mixing matrix," *JCAP* **07** (2019) 014, [[arXiv:1905.11290](#) [astro-ph.CO]].
- [46] J. Froustey, C. Pitrou, and M. C. Volpe, "Neutrino decoupling including flavour oscillations and primordial nucleosynthesis," *JCAP* **12** (2020) 015, [[arXiv:2008.01074](#) [hep-ph]].
- [47] J. J. Bennett, G. Buldgen, P. F. De Salas, M. Drewes, S. Gariazzo, S. Pastor, and Y. Y. Y. Wong, "Towards a precision calculation of  $N_{\text{eff}}$  in the Standard Model II: Neutrino decoupling in the presence of flavour oscillations and finite-temperature QED," *JCAP* **04** (2021) 073, [[arXiv:2012.02726](#) [hep-ph]].
- [48] M. Drewes, Y. Georis, M. Klasen, L. P. Wiggering, and Y. Y. Y. Wong, "Towards a precision calculation of  $N_{\text{eff}}$  in the Standard Model. Part III. Improved estimate of NLO contributions to the collision integral," *JCAP* **06** (2024) 032, [[arXiv:2402.18481](#) [hep-ph]].
- [49] V. A. Rubakov and D. S. Gorbunov, *Introduction to the Theory of the Early Universe: Hot big bang theory*. World Scientific, Singapore, 2017.
- [50] M. Viel, J. Lesgourgues, M. G. Haehnelt, S. Matarrese, and A. Riotto, "Constraining warm dark matter candidates including sterile neutrinos and light gravitinos with WMAP and the Lyman-alpha forest," *Phys. Rev. D* **71** (2005) 063534, [[arXiv:astro-ph/0501562](#)].
- [51] A. Boyarsky, J. Lesgourgues, O. Ruchayskiy, and M. Viel, "Lyman-alpha constraints on warm and on warm-plus-cold dark matter models," *JCAP* **05** (2009) 012, [[arXiv:0812.0010](#) [astro-ph]].
- [52] R. Murgia, A. Merle, M. Viel, M. Totzauer, and A. Schneider, "'Non-cold' dark matter at small scales: a general approach," *JCAP* **11** (2017) 046, [[arXiv:1704.07838](#) [astro-ph.CO]].
- [53] M. Drewes *et al.*, "A White Paper on keV Sterile Neutrino Dark Matter," *JCAP* **01** (2017) 025, [[arXiv:1602.04816](#) [hep-ph]].
- [54] M. Garny and J. Heisig, "Interplay of super-WIMP and freeze-in production of dark matter," *Phys. Rev. D* **98** no. 9, (2018) 095031, [[arXiv:1809.10135](#) [hep-ph]].
- [55] Q. Decant, J. Heisig, D. C. Hooper, and L. Lopez-Honorez, "Lyman- $\alpha$  constraints on freeze-in and superWIMPs," *JCAP* **03** (2022) 041, [[arXiv:2111.09321](#) [astro-ph.CO]].
- [56] A. Ringwald and Y. Y. Y. Wong, "Gravitational clustering of relic neutrinos and implications for their detection," *JCAP* **12** (2004) 005, [[arXiv:hep-ph/0408241](#)].
- [57] S. Weinberg, "Baryon and Lepton Nonconserving Processes," *Phys. Rev. Lett.* **43** (1979) 1566–1570.
- [58] T. Yanagida, "Horizontal gauge symmetry and masses of neutrinos," *Conf. Proc. C* **7902131** (1979) 95–99.